Inorg. Chem. **2007**, *46*, 4368–4370

Inorganic Chemistry
Communication

Ternary Iron(III) Complex Showing Photocleavage of DNA in the Photodynamic Therapy Window

Mithun Roy, Sounik Saha, Ashis K. Patra, Munirathinam Nethaji, and Akhil R. Chakravarty*

Department of Inorganic and Physical Chemistry, Indian Institute of Science, Bangalore 560012, India

Received October 27, 2006

A new ternary iron(III) complex [FeL(dpq)] containing dipyridoquinoxaline (dpq) and 2,2-bis(3,5-di-*tert*-butyl-2-hydroxybenzyl)aminoacetic acid (H_3L) is prepared and structurally characterized by X-ray crystallography. The high-spin complex with a FeN_3O_3 core shows a quasi-reversible iron(III)/iron(II) redox couple at –0.62 V (vs SCE) in DMF/0.1 M TBAP and a broad visible band at 470 nm in DMF/Tris buffer. Laser photoexcitation of this phenolate (L)-to-iron(III) charge-transfer band at visible wavelengths including red light of $\geq$630 nm leads to cleavage of supercoiled pUC19 DNA to its nicked circular form via a photoredox pathway forming hydroxyl radicals.

Photofrin is the clinically used drug in the photodynamic therapy (PDT) of lung and esophageal cancers.[1,2] It is a mixture of hematoporphyrin and its derivatives. The drug gets activated upon photoexcitation of the Q band at 630 nm. The photoactivation leads to the $^1\pi\pi^*$ state followed by formation of the triplet state $^3\pi\pi^*$ that activates $^3O_2$ to the cytotoxic $^1O_2$ by energy transfer. The porphyrin-based drugs suffer from dark toxicity. Besides, oxidative conversion of porphyrin bases to bilirubin leads to hepatotoxicity.[1] This drug has generated interests to search for and design new porphyrin and phthalocyanine bases[1,2a] as well as non-porphyrinic complexes of bioessential metal ions that could efficiently bind and cleave DNA in the PDT window of 600−800 nm. In this Communication, we report the first iron-based complex that shows efficient cleavage of plasmid DNA upon laser irradiation at red light.

Polypyridyl complexes of 4d transition metals like ruthenium and rhodium are known to cleave DNA upon photoirradiation.[3−5] We have reported copper(II) complexes showing DNA cleavage at red light.[6] The present work stems from our interest to design iron-based DNA photocleavers at visible light considering the bioessential nature of this element. While iron complexes are generally used in footprinting studies,[7] the only iron complex known[8] to cleave DNA upon photolysis up to 500 nm using its ligand-to-metal charge-transfer (LMCT) bands at 340 and 425 nm is reported by Kraft and Zaleski. The photoinitiated DNA cleavage takes place as a result of dinitrogen release from the tris(3-hydroxy-1,2,3-benzotriazine-4(3*H*)-one)iron(III) complex. We have designed a new ternary iron(III) complex [FeL(dpq)] (**1**) using dipyrido[3,2-*d*:2′,3′-*f*]quinoxaline (dpq) as a DNA binder and 2,2-bis(3,5-di-*tert*-butyl-2-hydroxybenzyl)aminoacetic acid (H_3L) as a ligand stabilizing the ferric state. Ligand dpq has a quinoxaline moiety like that in antitumor antibiotics echinomycin and triostin.[9] This work presents a new approach to designing iron-based photonucleases in the PDT window and provides direct spectral evidence of the involvement of the LMCT band in the photoexcitation process.

Complex **1**, prepared from the reaction of $Fe(NO_3)_3{\cdot}9H_2O$ with H_3L and dpq, has been structurally characterized by X-ray crystallography (Figure 1a).[10,11] The crystal structure displays the discrete mononuclear nature of **1**, where the ligand L^{3-} and dpq display respective tetradentate and bidentate chelating modes of binding to the iron(III) center in FeN_3O_3 coordination. The Fe−O and Fe−N bond distances are in the ranges of 1.904(4)−1.997(4) and 2.179(5)−2.352(5) Å, respectively. Two Fe−O(phenolate) dis-

* To whom correspondence should be addressed. E-mail: arc@ipc.iisc.ernet.in. Tel: 91-80-22932533. Fax: 91-80-23600683.

(1) Bonnet, R. *Chemical Aspects of Photodynamic Therapy*; Gordon & Breach: London, U.K., 2000.
(2) (a) Wei, W.-H.; Wang, Z.; Mizuno, T.; Cortez, C.; Fu, L.; Sirisawad, M.; Naumovski, L.; Magda, D.; Sessler, J. L. *Dalton Trans.* **2006**, 1934. (b) Henderson, B. W.; Busch, T. M.; Vaughan, L. A.; Frawley, N. P.; Babich, D.; Sosa, T. A.; Zollo, J. D.; Dee, A. S.; Cooper, M. T.; Bellnier, D. A.; Greco, W. R.; Oseroff, A. R. *Cancer Res.* **2000**, *60*, 525. (c) Sternberg, E. D.; Dolphin, D.; Brückner, C. *Tetrahedron* **1998**, *54*, 4151.
(3) (a) Metcalfe, C.; Thomas, J. A. *Chem. Soc. Rev.* **2003**, *32*, 215. (b) Szacilowski, K.; Macyk, W.; Drzewiecka-Matuszek, A.; Brindell, M.; Stochel, G. *Chem. Rev.* **2005**, *105*, 2647. (c) Armitage, B. *Chem. Rev.* **1998**, *98*, 1171.
(4) Chifotides, H. T.; Dunbar, K. R. *Acc. Chem. Res.* **2005**, *38*, 146.
(5) Erkkila, K. E.; Odom, D. T.; Barton, J. K. *Chem. Rev.* **1999**, *99*, 2777.
(6) (a) Dhar, S.; Senapati, D.; Das, P. K.; Chattopadhyay, P.; Nethaji, M.; Chakravarty, A. R. *J. Am. Chem. Soc.* **2003**, *125*, 12118. (b) Dhar, S.; Senapati, D.; Reddy, P. A. N.; Das, P. K.; Chakravarty, A. R. *Chem. Commun.* **2003**, 2452. (c) Patra, A. K.; Dhar, S.; Nethaji, M.; Chakravarty, A. R. *Chem. Commun.* **2003**, 1562.
(7) Routier, S.; Vezin, H.; Lamour, E.; Bernier, J.-L.; Catteau, J.-P.; Bailly, C. *Nucleic Acids Res.* **1999**, *27*, 4160.
(8) Kraft, B. J.; Zaleski, J. M. *New J. Chem.* **2001**, *25*, 1281.
(9) Toshima, K.; Takano, R.; Ozawa, T.; Matsumura, S. *Chem. Commun.* **2002**, 212.

10.1021/ic062056l CCC: $37.00
Published on Web 05/01/2007

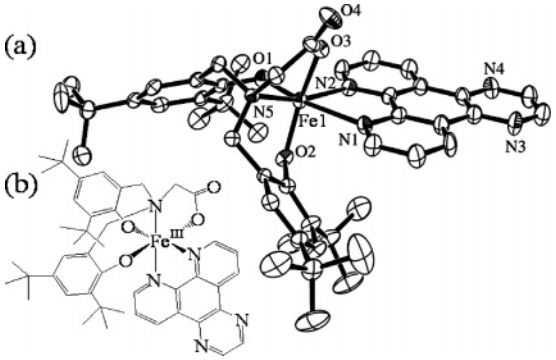

Figure 1. (a) ORTEP view of [FeL(dpq)] showing 30% probability thermal ellipsoids and a labeling scheme for the metal atoms and heteroatoms. (b) Schematic drawing of **1**.

tances are relatively short, while the Fe(1)−N(1) distance of 2.352(5) Å is significantly long. The Fe1−O1 bond distance is 1.904(4) Å. The structural features in **1** are similar to those reported for analogous 2,2′-bipyridine complexes.[12] The planar dpq ligand in **1** is sterically unhindered from the tetradentate ligand (L) having bulky *tert*-butyl groups.

Complex **1** shows a quasi-reversible cyclic voltammetric response at −0.62 V for the iron(III)/iron(II) couple in dimethylformamide (DMF) containing 0.1 M [(^{t}Bu)$_4$N](ClO$_4$) (ΔE_p = 95 mV at 50 mV s^{-1}). A high negative potential of the redox couple indicates stability of the ferric state. The complex shows a magnetic moment of 5.86 μ_B in the solid state at 298 K, suggesting a high-spin ($S = {}^5/_2$) electronic configuration of iron(III). The complex displays a broad visible electronic band at 470 nm in a DMF/Tris-HCl buffer. This band is assignable to the phenolate (p_π)-to-iron(III) (d_{π^*}) charge-transfer transition (Figure 2).[8,12] The 470 nm charge-transfer band is broad, extending to the PDT window. This has enabled us to use different visible wavelengths for photoactivation of **1** in a DNA-bound form (Figure 2). Moderately high ϵ values at $\lambda \geq 600$ nm make **1** suitable for photoinduced DNA cleavage studies at red light.

The DNA binding propensity of **1** is evaluated by the absorption spectral measurements, monitoring the change of

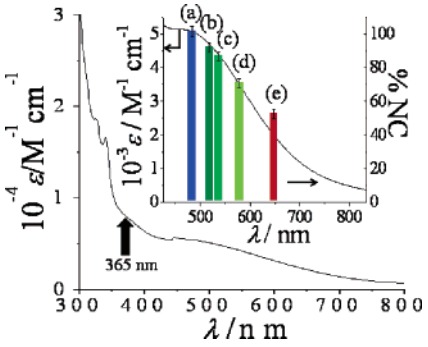

Figure 2. Electronic spectrum of **1** in a Tris-HCl buffer (pH 7.2) containing 6% DMF. The inset shows the extent of DNA cleavage by **1** at 476, 514, 532, 568, and 647 nm (a−e) upon LMCT band excitation using an argon−krypton laser.

the intensity of the spectral band at 253 nm with increasing concentration of calf thymus (CT) DNA.[13] The equilibrium binding constant (K_b) and the binding site size (s) of the complex are determined by the McGhee−von Hippel (MvH) method using the expression of Bard and co-workers.[14] The K_b and s values obtained from the nonlinear least-squares fitting are 2.1 (±0.3) × 10^5 M^{-1} and 0.71, respectively. The bulk of L with *tert*-butyl groups does not cause any major steric constraint on the DNA binding property. The K_b value compares well to those of metal complexes having polypyridyl ligands with extended aromatic rings.[15]

The photoinduced DNA cleavage activity of **1** is studied using supercoiled (SC) pUC19 DNA (33.3 μM bp, 0.2 μg) in a medium of a Tris-HCl/NaCl buffer (50 mM, pH, 7.2) upon irradiation with monochromatic UV light of 365 nm (12 W) and by laser at different visible wavelengths, viz., 476, 514, 532, 568, and 647 nm, using a continuous-wave (CW) argon−krypton laser of 100 mW power (Figure 3).[13] We have also studied the DNA cleavage activity of **1** at 632.8 nm with a helium−neon laser (12 mW) considering the photofrin activity at 630 nm.[1] A 5.6 μM solution of **1** completely cleaves SC DNA at 365 nm upon 2 h of photoexposure. The DNA binding property of **1** is studied using minor groove binder distamycin A, which alone gives ∼27% cleavage of SC DNA to its nicked circular form at 365 nm (Figure 3a, lane 7). The addition of **1** does not show any apparent change in the cleavage activity, indicating a DNA minor groove binding preference of **1** (Figure 3a, lane 8).

(10) The complex was prepared by reacting H_3L (0.24 g, 0.5 mM) taken in a mixture of MeOH, EtOH, and MeCN (3:3:2, v/v, 20 mL) with Et_3N (0.2 mL, 1.5 mM) followed by the addition of $Fe(NO_3)_3 \cdot 9H_2O$ (0.20 g, 0.5 mM). The solution was stirred for 15 min followed by the addition of dpq (0.12 g, 0.5 mM). It was filtered after 10 min. The filtrate upon slow concentration gave dark-purple block-shaped crystals in analytically pure form [yield: 0.27 g (65%)]. Anal. Calcd for $C_{46}H_{54}N_5O_4Fe \cdot MeCN$: C, 69.34; H, 6.83; N, 8.79. Found: C, 69.16; H, 6.95; N, 9.21. Λ_M = 10 S m^2 M^{-1}. FT-IR (KBr phase): 1670 cm^{-1} (ν_{COO^-}). ESI-MS: m/z 797.3 (M + H)$^+$. UV−visible in a 6% DMF/Tris-HCl buffer [λ_{max}, nm (ϵ, M^{-1} cm^{-1})]: 253 (71 720), 282 (39 770), 325 (18 680), 340 (16 600), 470 (5140). μ_{eff} (298 K): 5.86 μ_B.

(11) Crystal data for **1**·MeCN: $C_{48}H_{57}N_6O_4Fe$, M = 837.85, monoclinic, $P2_1/n$, a = 14.907(6) Å, b = 13.736(6) Å, c = 21.759(9) Å, β = 92.844(9)°, V = 4450(3) Å^3, Z = 4, ρ = 1.251 g cm^{-3}, T = 293(2) K, 1.70 ≤ θ ≤ 25.25°, μ = 3.89 cm^{-1}, F(000) = 1780, goodness-of-fit (GOF) = 1.042, R1 = 0.0927, wR2 = 0.1989 for 4526 reflections with $I > 2\sigma(I)$ and 523 parameters [R1(F^2) = 0.1635 (all data)]. $w = [\sigma^2(F_o^2) + (0.0869P)^2 + 8.7803P]^{-1}$, where $P = [F_o^2 + 2F_c^2]/3$ (Bruker SMART APEX CCD diffractometer with a Mo Kα X-ray source). The structure was solved and refined using the *SHELX* program (Sheldrick, G. M. *SHELX-97, Programs for Crystal Structure Solution and Refinement*; University of Göttingen: Göttingen, Germany, 1997).

(12) Shongwe, M. S.; Kaschula, C. H.; Adsetts, M. S.; Ainscough, E. W.; Brodie, A. M.; Morris, M. J. *Inorg. Chem.* **2005**, *44*, 3070.

(13) DNA binding and cleavage experiments were carried out using CT DNA (ca. 310 μM NP) and SC pUC19 DNA (0.2 μg, 33.3 μM bp), respectively, in a 5 mM Tris-HCl/5 mM NaCl buffer (pH 7.2) containing 6% DMF. The light sources used were a UV lamp of 365 nm (12 W), tunable wavelength Spectra Physics Water-Cooled Mixed-Gas Ion Laser Stabilite 2018-RM with laser power meter model 407A (100 mW, CW beam diameter at 1/e^2 = 1.8 mm ± 10%, beam divergence = 0.7 mrad ± 10%), and a CW helium−neon laser of Research Electro-Optics make (632.8 nm, 12 mW, beam diameter = 0.88 mm, beam divergence = 0.92 mrad). The complex and reagent concentrations correspond to those in the 18 μL sample volume (solution pathlength = 5 mm). The extent of DNA cleavage was measured from the intensities of the bands in agarose gels using a UVITECH Gel Documentation System.

(14) (a) McGhee, J. D.; von Hippel, P. H. *J. Mol. Biol.* **1974**, *86*, 469. (b) Carter, M. T.; Rodriguez, M.; Bard, A. J. *J. Am. Chem. Soc.* **1989**, *111*, 8901.

(15) Carlson, D. L.; Huchital, D. H.; Mantilla, E. J.; Sheardy, R. D.; Murphy, W. R., Jr. *J. Am. Chem. Soc.* **1993**, *115*, 6424.

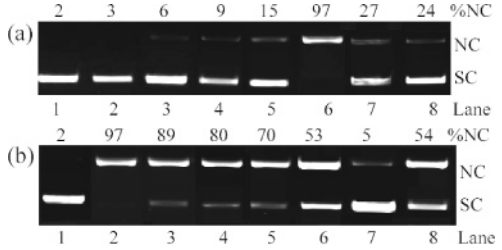

Figure 3. Gel electrophoresis diagrams showing cleavage of SC pUC19 DNA (0.2 μg, 33.3 μM bp) by [FeL(dpq)] (**1**) for 2 h of exposure time. (a) λ = 365 nm except for lane 5: lane 1, DNA control; lane 2, DNA + $Fe(NO_3)_3 \cdot 9H_2O$ (33.3 μM); lane 3, DNA + dpq (33.3 μM); lane 4, DNA + H_3L (33.3 μM); lane 5, DNA + **1** (33.3 μM) in dark (2 h); lane 6, DNA + **1** (5.6 μM); lane 7, DNA + distamycin A (2 units); lane 8, DNA + distamycin A (2 units) + **1** (5.6 μM). (b) At visible wavelengths: lane 1, DNA control (476 nm); lane 2, DNA + **1** (476 nm); lane 3, DNA + **1** (514 nm); lane 4, DNA + **1** (532 nm); lane 5, DNA + **1** (568 nm); lane 6, DNA + **1** (647 nm); lane 7, DNA control (632.8 nm); lane 8, DNA + **1** (632.8 nm) [complex concentration = 33.3 μM].

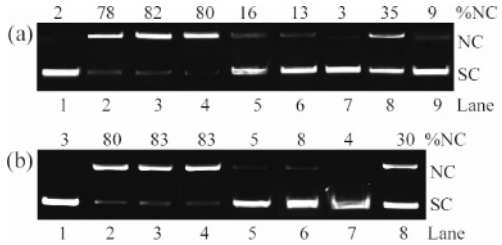

Figure 4. Gel electrophoresis diagrams showing cleavage of SC pUC19 DNA (0.2 μg, 33.3 μM bp) by **1** [5.6 μM at 365 nm; 33.3 μM at 476 nm]. (a) λ = 365 nm, exposure time (t) of 1 h: lane 1, DNA control; lane 2, DNA + **1**; lane 3, DNA + NaN_3 (22 μM) + **1**; lane 4, DNA + D_2O (14 μL) + **1**; lane 5, DNA + KI (22 μM) + **1**; lane 6, DNA + DMSO (4 μL) + **1**; lane 7, DNA + catalase (2 units) + **1**; lane 8, DNA + SOD (2 units) + **1**; lane 9, DNA + **1** (under argon; t = 2 h). (b) λ = 476 nm, t = 1 h: lane 1, DNA control; lane 2, DNA + **1**; lane 3, DNA + NaN_3 (133 μM) + **1**; lane 4, DNA + D_2O (14 μL) + **1**; lane 5, DNA + DMSO (5 μL) + **1**; lane 6, DNA + KI (133 μM) + **1**; lane 7, DNA + catalase (4 units) + **1**; lane 8, DNA + SOD (4 units) + **1**.

Scheme 1. Mechanism Proposed for the Photoinduced DNA Cleavage by **1**, Forming a Hydroxyl Radical in a Photoredox Pathway

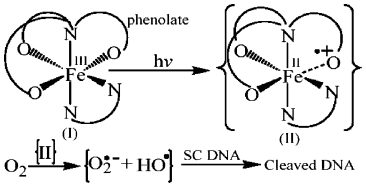

Control experiments with **1** in the dark or with H_3L, dpq, or $Fe(NO_3)_3 \cdot 9H_2O$ alone do not show any significant cleavage of SC DNA at 365 nm. When exposed to 476 nm CW argon−krypton laser (100 mW) for 2 h, 33.3 μM **1** completely cleaves SC DNA. To explore the possibility of the involvement of the LMCT band in the photoexcitation process, we have studied the DNA cleavage activity at longer wavelengths like 514, 532, 568, and 647 nm using the same laser (Figure 3b). Interestingly, the observed percent cleavage follows the spectral pattern (Figure 2). The complex shows ~50% cleavage at 647 nm red light. A similar percent cleavage is observed at 632.8 nm (helium−neon laser).

Mechanistic aspects of the photoinduced DNA cleavage reactions are studied at 365 and 476 nm (Figure 4). While **1** is cleavage-active in air, it is inactive under argon (Figure 4a). This indicates the involvement of molecular oxygen in the DNA photocleavage reaction. We have probed the cleavage activity using different external reagents. There is no apparent variation in the cleavage activity in the presence of singlet oxygen quencher sodium azide. The addition of deuterated water does not show any enhancement of the cleavage activity, thus ruling out a $^1O_2$ (type II) pathway. Hydroxyl radical scavangers dimethyl sulfoxide (DMSO), KI, and catalase show complete inhibition at both 365 and 476 nm. Superoxide scavenger superoxide dismutase (SOD) shows significant inhibition of the cleavage activity, indicating the formation of transient superoxide species (Figure 4a,b, lane 8).

Mechanistic data suggest a photoredox pathway in which **1** upon photoexcitation at the LMCT band forms a charge-separated $Fe^{2+}-L^{\bullet+}$ (phenolate ligand radical) intermediate involving the Fe−phenolato bond (Scheme 1).[8] Subsequent reactions with O_2 could lead to $O_2^{\bullet-}$ formation followed by the generation of $HO^{\bullet}$ in the reaction $3O_2^{\bullet-} + 2H^+ \rightarrow HO^{\bullet} + HO^- + 2O_2$ as reported[16] for antitumor natural product podophyllotoxin. Electron paramagnetic resonance (EPR) studies using 5,5-dimethyl-1-pyrroline *N*-oxide (DMPO) show DMPO−$HO^{\bullet}$ formation (Figure S7a in the Supporting Information). Anaerobic photoexcitation of **1** shows reduction in the LMCT band intensity that reverts back upon exposure to O_2 (Figure S8 in the Supporting Information).

In summary, we report here the first iron-based, low-molecular-weight complex that shows efficient DNA binding and cleavage activity at red light. We provide here direct spectral evidence of the involvement of the LMCT band in the metal-assisted photosensitization process. The percent of DNA cleavage at different wavelengths follows the visible spectral pattern. The oxidative DNA cleavage proceeds via a photoredox pathway, forming a hydroxyl radical as the DNA-cleavage-active species. This is in contrast to the porphyrin and related bases cleaving DNA by a singlet oxygen mechanism. The present work opens up new avenues for designing and developing iron-based compounds for possible use in PDT chemistry.

Acknowledgment. We thank the Department of Science and Technology (DST, Government of India) and the Council of Scientific and Industrial Research (CSIR, New Delhi, India) for financial support and the DST for use of the CCD diffractometer facility. We also thank the Alexander von Humboldt Foundation, Germany, for donation of an electroanalytical system. A.K.P. and S.S. are thankful to CSIR for their fellowships.

Supporting Information Available: Crystallographic details in CIF format, ORTEP, unit cell packing, and space-filling diagrams (Figures S1−S3), electrospray ionization mass spectrum (Figure S4), cyclic volatmmogram (Figure S5), DNA binding, EPR, UV−visible, and gel electrophoresis diagrams (Figures S6−S10), and Scheme S1. This material is available free of charge via the Internet at http://pubs.acs.org.

IC062056L

(16) Sakurai, H.; Miki, T.; Imakura, Y.; Shibuya, M.; Lee, K.-H. *Mol. Pharmacol.* **1991**, *40*, 965.